


Superconductivity of neutral modes in quantum Hall edges

Jukka I. Värynen¹, Moshe Goldstein², and Yuval Gefen³

¹*Department of Physics and Astronomy, Purdue University, West Lafayette, Indiana 47907, USA*

²*Raymond and Beverly Sackler School of Physics and Astronomy, Tel Aviv University, Tel Aviv 6997801, Israel*

³*Department of Condensed Matter Physics, Weizmann Institute of Science, Rehovot 76100, Israel*

 (Received 16 June 2021; revised 28 December 2021; accepted 25 January 2022; published 3 February 2022)

The edges of quantum Hall phases give rise to a multitude of exotic modes supporting quasiparticles of different values of charge and quantum statistics. Among these are neutralons (chargeless anyons with semion statistics), which were found to be ubiquitous in fractional quantum Hall matter. Studying and manipulating the neutral sector is an intriguing and interesting challenge, all the more so since these particles are accessible experimentally. Here, we address the limit of strongly interacting neutralons giving rise to neutralon superconductivity, where pairing is replaced by a quarteting mechanism. We discuss several manifestations of this effect, realizable in existing experimental platforms. Furthermore, this superconducting gapping mechanism may be exploited to facilitate the observation of interference of the accompanying charged anyons.

DOI: [10.1103/PhysRevB.105.L081402](https://doi.org/10.1103/PhysRevB.105.L081402)

Introduction. A two-dimensional electron gas in a fractional quantum Hall (FQH) state can host exotic anyonic quasiparticles and boundary modes [1–5]. The boundary modes may be used as building blocks for realizing anyonic transport and designing interference experiments to observe fractional quantum statistics beyond bosons and fermions [6]. Major recent experimental developments involve the observation [7] of Hong-Ou-Mandel [8–11] anyonic correlations as well as a demonstration [12] of anyonic interferometry [13–20].

Some of the exotic boundary modes arise as renormalized bare edge modes. Examples include neutral modes which have been experimentally detected through thermometry [21] and the generation of upstream charge noise [22–26]. The paradigmatic model of gapless neutral modes was introduced by Kane, Fisher, and Polchinski (KFP) [27] for the $\nu = 2/3$ FQH edge which hosts counterpropagating $\nu = 1$ and $\nu = 1/3$ chiral bare modes [28,29]. Random backscattering and Coulomb interactions between the modes drive the edge to a new low-energy fixed point that hosts a charge- $2e/3$ mode and a counterpropagating “upstream” neutral mode. In the original KFP model the neutral modes satisfy SU(2) symmetry, but more complex edges (for example, due to edge reconstruction) may give rise to more elaborate structures such as SU(3) symmetric modes [30].

So far these studies have focused on noninteracting neutral modes. Exploring the physics of interacting neutral mode system opens the door to new exotic phases. Here, we show that interactions within the neutral mode sector may give rise to *neutralon superconductivity*, relying on amalgamating (hereafter “pairing”) together a quartet of neutral quasiparticles.

The neutral modes are chiral, so in order to open a superconducting gap, a counterpropagating partner needs to be introduced [31]. Here, we take advantage of a recent material engineering breakthrough [32] and theoretically investigate a

suitably designed FQH bilayer, where two counterpropagating copies of the $\nu = 2/3$ FQH neutral mode appear (see also Ref. [33]). We start from the limit of weak neutralon-neutralon interactions. In that limit, in the presence of disorder-induced tunneling between the counterpropagating neutralons, Anderson localization is suppressed [34], and hence will not compete against opening a superconducting gap. Uniform backscattering competes with uniform pairing, both being marginal operators (for weak interactions). However, neutralons are charge dipoles, hence subject to a weak attractive density-density interaction $v_{0,0}$ which favors pairing. Interestingly, due to the semionic nature of neutralons, the pairing must involve four of them. This pairing conserves momentum and is marginally relevant even in the presence of edge disorder. We use perturbative renormalization group to infer properties of the strongly coupled neutralons in the low-temperature limit.

Superconductivity in the neutral sector has experimental manifestations that involve measurements of the charge modes. The tunneling of electrons across a quantum point contact bridging fractional quantum Hall states will generally excite neutral modes. When the neutral modes are gapped by pairing, electron tunneling is highly suppressed at low energies, which may be observed in the low-bias I - V characteristics and the shot noise Fano factor. Another signature involves a confined quantum dot or antidot geometry, where unpaired neutralons come at a cost of pairing energy, which is manifest in Coulomb blockade peak spacings [35].

Furthermore, our analysis concerns the design of anyonic interferometers. It is known that gapless neutralons may act as “which-path” detectors. Their ubiquity [26,36] leads to dephasing, hence suppression of interference [37]. We therefore propose that when neutralons condense to a gapped state, the sensitivity of anyonic interferometry will improve. Below, we outline interferometer designs that could be used to gap out

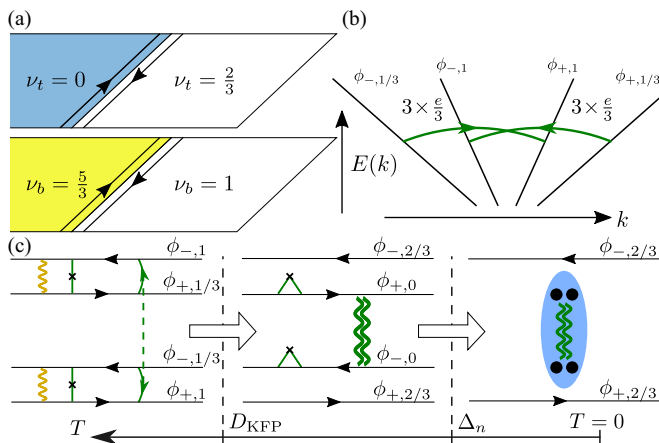


FIG. 1. (a) Bilayer FQH structure where neutralons can be gapped. We consider an interface where both the bottom and top layers of the structure have an interface described by the KFP theory for the $\nu = 2/3$ FQH state. The filling fractions are chosen in a way that produces opposite spin polarizations for the top and bottom layers. (b) Edge spectrum of the clean limit. Correlated intralayer backscattering process (green curved arrows) that contributes to pairing of neutralons at low energies. (c) The characteristic temperature scales and the two-step RG flow towards low temperature (large white arrows). The bare edge modes at high temperatures on the left, with a Coulomb interaction (yellow wiggly line), random backscattering (solid line with a cross), and correlated intralayer backscattering (curved arrows connected by a dashed line). As temperature is lowered below D_{KFP} , the edge is described by the KFP low-energy theory (middle panel) of $2e/3$ charge modes and disordered neutral modes with a pairing interaction (green wiggly double line line). At temperatures below Δ_n , quartets of neutralons become gapped (blue ellipse) and only the charge modes remain (right panel). Their opposite spin polarization prevents backscattering.

the harmful neutralons while leaving the charge excitations gapless, thus improving interferometer performance. The observation of a superconducting neutralon phase may have far-reaching impacts on the quest for anyonic interference.

Our theoretical analysis follows these steps: We will consider a bilayer of counterpropagating neutral modes. The latter are represented by bosonic fields as described in the original work by KFP [27]. The corresponding action, Eq. (3), is derived without interlayer tunneling. We then include weak interlayer perturbations, pairing and backscattering [see Eq. (5)]. Employing the perturbative renormalization group, we identify the parameter regime where pairing becomes the most relevant perturbation. The energy scale at which pairing becomes nonperturbative (strongly coupled) is the superconducting gap Δ_n , at energies below which the pairing interaction leads to a *quartet superconductivity*. Finally, we discuss the experimental manifestations of the superconducting phase.

Model of a single edge. We start from the description of a single composite interface depicted in Fig. 1(a). Both the top and bottom components have an interface similar to a $\nu = 2/3$ edge. Assuming spin-polarized Landau levels, our edge theory therefore consists of four chiral bosonic fields $\phi_{+,1/3,\uparrow}, \phi_{-,1,\uparrow}, \phi_{-,1/3,\downarrow}, \phi_{+,1,\downarrow}$ where the subscripts indicate

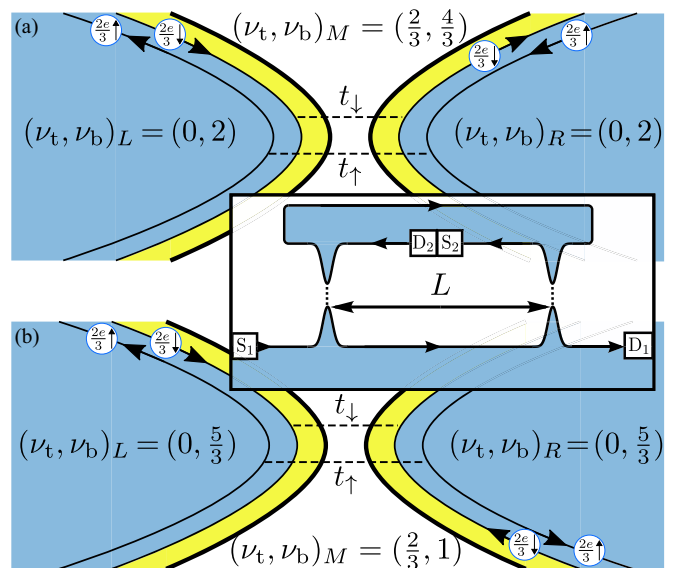


FIG. 2. Two quantum point contact (QPC) designs showing the composite edge of Fig. 1(a) from the top. For the sake of clarity, we have shifted the top and bottom layers laterally. Both sides of the QPC are at the fixed point where neutral modes are localized. Each side therefore hosts a helical pair of $2e/3$ charge modes with a spin up (down) mode living on the bottom (top) layer of the double quantum well. Tunneling across the QPC is assumed to conserve the spin eigenvalue. The figures show two different setups: In (a) the top layer quasiparticles tunnel through a $\nu = 2/3$ bulk rather than a trivial vacuum (in the bottom layer tunneling is through a $\nu = 1$ trivial vacuum). In (b), in both layers quasiparticles tunnel through a fractional $\nu = 2/3$ vacuum. These two setups have different zero-bias anomalies in the tunneling current and different shot noise Fano factors. Inset: A Mach-Zehnder interferometer is not susceptible to dephasing from neutral modes provided its linear size L exceeds the neutral mode decay length, $L \gg \nu_0/\Delta_n$, and the bias voltage is low, $eV \ll \Delta_n$.

the chirality (“+” denotes a right mover), charge, and spin. The imaginary time action is [27] (a is a short-distance cutoff)

$$S^{(0)} = \int d\tau dx \frac{1}{4\pi} [\partial_x \Phi \mathbf{K} i \partial_\tau \Phi + \partial_x \Phi \mathbf{V} \partial_x \Phi] + \frac{1}{a} \int d\tau dx \sum_{l=t,b} [\xi_l(x) e^{i\mathbf{c}_l \cdot \Phi_l} + \xi_l^*(x) e^{-i\mathbf{c}_l \cdot \Phi_l}], \quad (1)$$

where we introduced the four-component vector $\Phi = (\phi_t, \phi_b) = (\phi_{+,1/3,\uparrow}, \phi_{-,1,\uparrow}, \phi_{-,1/3,\downarrow}, \phi_{+,1,\downarrow})$. In this basis the matrix \mathbf{V} is almost block-diagonal [38], describing the velocities and short-range screened Coulomb interactions between the modes; the matrix $\mathbf{K} = \text{diag}(3, -1, -3, 1)$ describes the commutation relations [39]. We may use the same action to describe other interfaces such as those depicted in Fig. 2 [38]. On the second line of Eq. (1) we have included random intralayer backscattering of electrons between the counterpropagating $1/3$ and 1 modes; here, $\mathbf{c}_{t(b)} = (-1)(3, 1)$ and ξ_l is a δ -correlated random coefficient, $\langle \xi_l(x) \xi_l^*(x') \rangle = a^{-1} W_l \delta(x - x')$, with zero average. This term is a relevant perturbation under the renormalization group [40] (RG) and leads to a nontrivial renormalization of the edge theory [27].

In Eq. (1) we neglect interlayer perturbations which will be included later [see Eq. (5)].

Below a temperature scale $T \sim D_{\text{KFP}}$, the disorder strength W_l becomes large [41] and the edge action can be diagonalized in terms of spinless neutralons and spinful charge- $2e/3$ modes given by the respective linear combinations [Fig. 1(a)],

$$\begin{aligned}\phi_{+,0} &= \frac{3\phi_{+,1/3,\uparrow} + \phi_{-,1,\uparrow}}{\sqrt{2}}, \\ \phi_{-,2/3,\uparrow} &= \sqrt{\frac{3}{2}}[\phi_{+,1/3,\uparrow} + \phi_{-,1,\uparrow}],\end{aligned}\quad (2)$$

and similarly for the bottom edge. Introducing $\phi = (\phi_{+,2/3,\downarrow}, \phi_{-,2/3,\uparrow}, \phi_{+,0}, \phi_{-,0})$, the low-energy action is

$$\begin{aligned}S_{\text{KFP}}^{(0)} &= \int d\tau dx \frac{1}{4\pi} [\partial_x \phi \mathbf{K}_{\text{KFP}} i\partial_\tau \phi + \partial_x \phi \mathbf{V}_{\text{KFP}} \partial_x \phi] \\ &+ \frac{1}{a} \int d\tau dx [\xi_a(x) e^{i\sqrt{2}\phi_{+,0}} + \xi_b(x) e^{-i\sqrt{2}\phi_{-,0}} + \text{H.c.}],\end{aligned}\quad (3)$$

with $\mathbf{K}_{\text{KFP}} = \text{diag}(1, -1, 1, -1)$ and \mathbf{V}_{KFP} is a block-diagonal matrix. The block diagonality of \mathbf{V}_{KFP} is a result of the random intralayer backscattering, which makes neutralon-chargeon interactions $\partial_x \phi_{\pm,0}, \partial_x \phi_{\pm,2/3}$ irrelevant [27]. However, \mathbf{V}_{KFP} includes a neutralon-neutralon interaction $v_{0,0}$ which is not irrelevant for layer-correlated disorder (considered below) [38]. The second line in Eq. (3) introduces random phases into the neutral sector but does not give rise to a gap [27]. We note that the operators $e^{\pm i\sqrt{2}\phi_{\pm,0}}$ create two neutralons on the edge [38]. A combination of these operators creates a quartet of counterpropagating neutralons and can open a superconducting gap.

Interlayer tunneling. Let us next include weak interlayer tunneling to the action $S_{\text{KFP}}^{(0)}$ [Eq. (3)]. This introduces the leading (in the RG sense) perturbations in the neutral sector: pairing [depicted in Fig. 1(b)], $O_p = e^{i\sqrt{2}[\phi_{+,0} - \phi_{-,0}]}$, and backscattering, $O_b = e^{i\sqrt{2}[\phi_{+,0} + \phi_{-,0}]}$. In the absence of neutral-neutral interactions ($v_{0,0} = 0$), both operators have a scaling dimension $\delta = 2$ and they are thus marginal (to leading order) as homogeneous perturbations [34]. In this case, the perturbation with a larger bare amplitude becomes the marginally relevant perturbation, as can be seen from Eqs. (6) and (7) below. However, for $v_{0,0} \neq 0$, the relevant operator is determined by the sign of $v_{0,0}$: For negative (positive) $v_{0,0}$, pairing (backscattering) becomes relevant while backscattering (pairing) becomes irrelevant. The relevant pairing term gives rise to a gap in the neutralon spectrum, $\Delta_n \approx D_{\text{KFP}} |\lambda_p|^{v_{0,0}/(2|v_{0,0}|)}$, in the limit $\lambda_p \ll |v_{0,0}|/v_0 \ll 1$ where λ_p is the dimensionless pairing amplitude [38,42] and v_0 is the neutral mode velocity. We show below that in the case when $v_{0,0}/v_0$ is comparable to the pairing and backscattering amplitudes, all three interactions get significantly renormalized but the general conclusion of a gap remains. The backscattering operator does not conserve momentum (unlike pairing), and is expected to be less relevant when the neutralons have a finite density [as depicted in Fig. 1(b)].

In the charge sector, backscattering is forbidden by spin conservation. The pairing of the charge modes is highly irrel-

evant [43] and also forbidden by charge conservation in the absence of an external superconductor [44].

Next, we will analyze the interlayer pairing O_p and backscattering O_b in the neutral sector. It is convenient to introduce the $\text{SU}(2)_1$ current operators [27,45]

$$\begin{aligned}J_\tau^z &= \frac{1}{2\pi\sqrt{2}} \partial_x \phi_{\tau,0}, & J_\tau^\pm &= \frac{1}{2\pi a} e^{\pm i\tau\sqrt{2}\phi_{\tau,0}}, \\ \tau &= t/b = +/-, & &\end{aligned}\quad (4)$$

and $J_\tau^\pm = J_\tau^x \pm iJ_\tau^y$. In terms of the currents, we have $O_p = 2\pi a J_\tau^+ J_\tau^+$ and $O_b = 2\pi a J_\tau^+ J_\tau^-$. We note that J_τ^+ creates a pair of neutralons on the τ edge [38]; the operator O_p therefore corresponds to a quarteting of neutralons. We can write the combined neutralon interlayer Hamiltonian in the form

$$H_{p+b} = 2\pi v_0 \int dx \sum_{i=x,y,z} \lambda^i J_i^i J_b^i, \quad (5)$$

where $\lambda^x = \lambda_p + \lambda_b$, $\lambda^y = \lambda_b - \lambda_p$ and λ_p, λ_b are the dimensionless pairing and backscattering amplitudes, and v_0 is the neutralon velocity. The neutralon density-density interaction from Eq. (3) is included in the ZZ term, $\lambda_0^z = 2v_{0,0}/v_0$. Upon reducing the bandwidth, these coupling constants get renormalized. In the absence of disorder [the second line in Eq. (3)], the perturbative RG equations for $\lambda^{i=x,y,z}$ are [46]

$$\frac{d}{dl} \lambda^x = \lambda^y \lambda^z, \quad \frac{d}{dl} \lambda^y = \lambda^x \lambda^z, \quad (6)$$

$$\frac{d}{dl} \lambda^z = \lambda^x \lambda^y \quad (l = \ln D_{\text{KFP}}/D), \quad (7)$$

where $D \ll D_{\text{KFP}}$ is the reduced bandwidth. We solve the above equations for $\lambda^i(D)$ with the initial condition $\lambda(D_{\text{KFP}}) = (\lambda_p + \lambda_b, \lambda_b - \lambda_p, \lambda_0^z)^T$. In the case $\lambda_0^z = 0$, we note that a nonzero λ^z is generated by Eq. (7), with a sign given by the sign of $\lambda_b^2 - \lambda_p^2$. In this case the low-temperature fixed point corresponds to the perturbation with the stronger bare coupling. However, physically we expect λ_0^z to be larger than λ_b, λ_p , since the former does not require interlayer tunneling. In this limit, the sign of λ_0^z determines the low-energy RG fixed point: When $\lambda_0^z > 0$, the fixed point corresponds to strong backscattering ($\lambda^x = \lambda^y = \pm \lambda^z$), while if $\lambda_0^z < 0$, the fixed point is of strong-pairing type ($\lambda^x = -\lambda^y = \pm \lambda^z$). Within each type, the fixed point is further determined by the sign of λ_b or λ_p : For example, in the strong-pairing case $\lambda_p > 0$ flows to ($\lambda^x = -\lambda^y = -\lambda^z > 0$) while $\lambda_p < 0$ flows to ($\lambda^x = -\lambda^y = +\lambda^z < 0$).

To estimate the strong-coupling energy scale Δ_n , we set $|\lambda^i(\Delta_n)| \gg 1$. We find $\Delta_n \approx D_{\text{KFP}} (2 \frac{|\lambda_0^z|}{|\lambda_p|})^{-\frac{1}{|v_{0,0}|}}$ in the limit $|\lambda_p| \ll |\lambda_0^z| \ll 1$ and $\Delta_n \approx D_{\text{KFP}} e^{-\pi/2|\lambda_p|}$ in the limit $|\lambda_0^z| \ll |\lambda_p| \ll 1$ [38]. At temperatures $T \ll \Delta_n$, the neutral excitations are gapped and only the charge modes remain from Eq. (3) [40]. Next, we will show that the random terms $\propto \xi_i(x), \xi_b(x)$ in Eq. (3) do not modify our conclusions.

Interpreting the current operators $\mathbf{J}_{t,b}$ as spin densities, the second line of Eq. (3) can be regarded as a random ‘‘in-plane magnetic field’’; the Hamiltonian corresponding to Eq. (3)

reads

$$H_{\text{neutral}} = 2\pi \sum_{\tau=t,b} \int dx \left(\frac{1}{3} v_0 \mathbf{J}_\tau^2 + \xi_\tau(x) J_\tau^+ + \xi_\tau^*(x) J_\tau^- \right). \quad (8)$$

The random magnetic field can be canceled by the following gauge transformation, that preserves the $SU(2)_1$ algebra [45] for $\tau = t, b$,

$$J_\tau^i = S_\tau^{ij} \tilde{J}_\tau^j + \frac{1}{8\pi} \varepsilon^{ijk} [S_\tau \partial_x S_\tau^T]^{jk}, \quad (9)$$

where $S_\tau(x)$ is a suitably chosen [38] real orthogonal matrix. For generic disorder, Eq. (9) does not keep the pairing term invariant and finding the ground state configuration is difficult. However, in the simple and realistic case of layer-correlated disorder, $\xi_t = \xi_b^* \equiv \xi$, we have [38,47]

$$\mathbf{J}_t^T \boldsymbol{\eta} \mathbf{J}_b = \tilde{\mathbf{J}}_t^T \boldsymbol{\eta} \tilde{\mathbf{J}}_b, \quad \text{where } \boldsymbol{\eta} = \text{diag}(1, -1, -1). \quad (10)$$

Thus, the rotation (9) makes the Hamiltonian independent of disorder,

$$H_{\text{neutral}} + H_{\text{pairing}} = 2\pi v_0 \int dx \left[\frac{1}{3} \sum_{\tau=t,b} \tilde{\mathbf{J}}_\tau^2 + \lambda \tilde{\mathbf{J}}_t^T \boldsymbol{\eta} \tilde{\mathbf{J}}_b \right], \quad (11)$$

as long as we have $\lambda = (\lambda, -\lambda, -\lambda)^T$ in Eq. (5). We can therefore use Eqs. (6) and (7), derived in the absence of disorder, to study Eq. (11). With $\lambda > 0$, we find a strong-pairing RG fixed point which preserves the direction of the vector λ . We expect that the fixed point with $\lambda < 0$ is similarly stable to disorder [38].

We have shown that, under certain assumptions, the disorder term in Eq. (8) can be gauged away and the same low-energy fixed points as in the clean system can be reached. When $\lambda_0^z < 0$, we identified two stable strong-pairing fixed points corresponding to $\lambda^x > 0$ and $\lambda^x < 0$. Next, we study the low-energy properties of the charge excitations near a fixed point where the neutralons are paired.

Experimental manifestations. The gapping of neutral modes at low energies has a number of implications to transport experiments. Signatures of a neutral mode gap can be found in tunneling across a QPC (see Fig. 2). Tunneling of fractional charge between the charge- $2e/3$ eigenmodes at low-bias voltage may be impeded in several ways depending on the filling factors of the left and right sides of the QPC as well as the filling $(\nu_l, \nu_r)_M$ of the middle section. Most conducive to fractional charge tunneling is having fractional $(\nu_l, \nu_r)_M$ [see Fig. 2(a)]; in that case the tunneling of $2e/3$ and $e/3$ quasiparticles is allowed. The latter involves the gapped neutralons and is thus suppressed (similarly to the case of charge- e tunneling discussed below) but the former is not. Indeed, the tunneling operator $O_{2/3,\uparrow} = e^{-i\sqrt{\frac{2}{3}}\phi_{-2/3,\uparrow,L}} e^{i\sqrt{\frac{2}{3}}\phi_{-2/3,\uparrow,R}}$ creates (annihilates) a charge- $2e/3$ eigenmode on the right (left) side of the QPC. The scaling dimension of $O_{2/3,\uparrow}$ is $\delta = 2/3$ and the tunneling current shows the corresponding zero-bias anomaly, $I \propto V^{2\delta-1}$ (keeping $eV \gg T$). The fractional tunneling charge also has a noise signature [8,48,49]: Tunneling charges $2e/3$ leads to a shot noise Fano factor $2/3$.

Tunneling is much more restricted when the middle region consists of an integer filling fraction state [cf. ν_b in the middle section of Fig. 2(b)]. In this case, only electrons (charge- e) are allowed to tunnel through the middle section. However, tunneling single electrons would excite the neutral modes and therefore come at a high-energy cost of order [35] Δ_n (for voltage bias $eV \ll \Delta_n$). The tunneling of a pair of electrons (three charge- $2e/3$ quasiparticles) does not excite the neutrals and is allowed. (Also, tunneling of a ‘‘Cooper pair’’ of counterpropagating neutralons would be allowed but will not transfer charge.) The tunneling of a pair of electrons has a scaling dimension $\delta = 4$, suppressing the tunneling current at low bias, $I \propto V^7$. Thus, when the tunnel barrier (in either bottom or top layer) has an integer filling fraction state, the low-bias tunneling current becomes highly suppressed. The tunneling current shot noise Fano factor in this case is expected to be 2, yet its observation may be challenging due to the smallness of the current. Gapped neutralons cannot propagate along the edge and thus are not expected to produce noise. Complementary signatures of neutralon pairing can be found in Coulomb blocked quantum dots or antidots [35] or in Andreev reflection of neutralons (see Ref. [38]).

The bilayer geometry where the neutral modes become gapped allows one to consider anyonic Mach-Zehnder or Fabry-Perot interferometers free of neutral mode dephasing (cf. Fig. 2). As discussed above, the configurations with fractional filling factors $(\nu_l, \nu_r)_M$ depicted in Fig. 2(a) are most suitable for constructing such an interferometer since they allow the tunneling of fractional charge quasiparticles. The size of the neutral mode gap Δ_n imposes some limitations to the interferometer design. For example, the distance L between the QPCs should be large enough, $L \gg v_0/\Delta_n$, and the bias voltage low enough, $eV \ll \Delta_n$, so that neutral modes cannot propagate through the interferometer causing dephasing. To observe interference, the length of the edge should not exceed the full incoherence length scale [45].

Discussion. We showed that counterpropagating neutral modes in a suitably designed FQH interface can be renormalized to a superconducting phase with a neutralon quartet pairing. We focused on engineered bilayer interfaces whose edge structure is similar to the $\nu = 2/3$ KFP edge theory [27]. In this case, the neutralons are semions and the superconductivity arises from neutralon quarteting. We expect our mechanism to also apply to reconstructed edges with emergent chiral modes [30] and other filling fractions, as long as these edges come with counterpropagating neutral modes. With different types of edge structures other unconventional neutralon statistics may arise, and we anticipate even more exotic (superconducting) phases of strongly interacting neutralon matter.

Acknowledgments. We thank Jinhong Park for useful discussions. M.G. was supported by the Israel Science Foundation (Grant No. 227/15) and the U.S.-Israel Binational Science Foundation (Grant No. 2016224). Y.G. was supported by DFG RO 2247/11-1, MI 658/10-2, and CRC 183 (project C01), the Minerva Foundation, the German Israeli Foundation (GIF I-1505-303.10/2019), the Helmholtz International Fellow Award, and by the Italia-Israel QUANTRA grant.

- [1] J. Leinaas and J. Myrheim, *Nuovo Cimento B* **37**, 1 (1977).
- [2] F. Wilczek, *Phys. Rev. Lett.* **49**, 957 (1982).
- [3] R. B. Laughlin, *Phys. Rev. Lett.* **50**, 1395 (1983).
- [4] B. I. Halperin, *Phys. Rev. Lett.* **52**, 1583 (1984).
- [5] D. Arovas, J. R. Schrieffer, and F. Wilczek, *Phys. Rev. Lett.* **53**, 722 (1984).
- [6] D. E. Feldman and B. I. Halperin, *Rep. Prog. Phys.* **84**, 076501 (2021).
- [7] H. Bartolomei, M. Kumar, R. Bisognin, A. Marguerite, J.-M. Berroir, E. Bocquillon, B. Plaças, A. Cavanna, Q. Dong, U. Gennser *et al.*, *Science* **368**, 173 (2020).
- [8] I. Safi, P. Devillard, and T. Martin, *Phys. Rev. Lett.* **86**, 4628 (2001).
- [9] G. Campagnano, O. Zilberberg, I. V. Gornyi, D. E. Feldman, A. C. Potter, and Y. Gefen, *Phys. Rev. Lett.* **109**, 106802 (2012).
- [10] G. Campagnano, O. Zilberberg, I. V. Gornyi, and Y. Gefen, *Phys. Rev. B* **88**, 235415 (2013).
- [11] B. Rosenow, I. P. Levkivskiy, and B. I. Halperin, *Phys. Rev. Lett.* **116**, 156802 (2016).
- [12] J. Nakamura, S. Liang, G. Gardner, and M. Manfra, *Nat. Phys.* **16**, 931 (2020).
- [13] C. de C. Chamon, D. E. Freed, S. A. Kivelson, S. L. Sondhi, and X. G. Wen, *Phys. Rev. B* **55**, 2331 (1997).
- [14] A. Stern and B. I. Halperin, *Phys. Rev. Lett.* **96**, 016802 (2006).
- [15] P. Bonderson, A. Kitaev, and K. Shtengel, *Phys. Rev. Lett.* **96**, 016803 (2006).
- [16] E. Grosfeld, S. H. Simon, and A. Stern, *Phys. Rev. Lett.* **96**, 226803 (2006).
- [17] K. T. Law, D. E. Feldman, and Y. Gefen, *Phys. Rev. B* **74**, 045319 (2006).
- [18] E.-A. Kim, *Phys. Rev. Lett.* **97**, 216404 (2006).
- [19] D. E. Feldman, Y. Gefen, A. Kitaev, K. T. Law, and A. Stern, *Phys. Rev. B* **76**, 085333 (2007).
- [20] B. Rosenow and A. Stern, *Phys. Rev. Lett.* **124**, 106805 (2020).
- [21] V. Venkatachalam, S. Hart, L. Pfeiffer, K. West, and A. Yacoby, *Nat. Phys.* **8**, 676 (2012).
- [22] A. Bid, N. Ofek, H. Inoue, M. Heiblum, C. L. Kane, V. Umansky, and D. Mahalu, *Nature (London)* **466**, 585 (2010).
- [23] M. Dolev, Y. Gross, R. Sabo, I. Gurman, M. Heiblum, V. Umansky, and D. Mahalu, *Phys. Rev. Lett.* **107**, 036805 (2011).
- [24] Y. Gross, M. Dolev, M. Heiblum, V. Umansky, and D. Mahalu, *Phys. Rev. Lett.* **108**, 226801 (2012).
- [25] I. Gurman, R. Sabo, M. Heiblum, V. Umansky, and D. Mahalu, *Nat. Commun.* **3**, 1289 (2012).
- [26] H. Inoue, A. Grivnin, Y. Ronen, M. Heiblum, V. Umansky, and D. Mahalu, *Nat. Commun.* **5**, 4067 (2014).
- [27] C. L. Kane, M. P. A. Fisher, and J. Polchinski, *Phys. Rev. Lett.* **72**, 4129 (1994).
- [28] A. H. MacDonald, *Phys. Rev. Lett.* **64**, 220 (1990).
- [29] X. G. Wen, *Phys. Rev. Lett.* **64**, 2206 (1990).
- [30] J. Wang, Y. Meir, and Y. Gefen, *Phys. Rev. Lett.* **111**, 246803 (2013).
- [31] X.-G. Wen, *Quantum Field Theory of Many-Body Systems* (Oxford University Press, Oxford, UK, 2004).
- [32] Y. Ronen, Y. Cohen, D. Banitt, M. Heiblum, and V. Umansky, *Nat. Phys.* **14**, 411 (2018).
- [33] Y. Wang, V. Ponomarenko, Z. Wan, K. W. West, K. W. Baldwin, L. N. Pfeiffer, Y. Lyanda-Geller, and L. P. Rokhinson, *Nat. Commun.* **12**, 5312 (2021).
- [34] We note that neutralons are semions, hence the allowed backscattering process involves four neutralons, making it highly irrelevant at low energies [27,50]. (The scaling dimension of the neutralon backscattering operator is 2.)
- [35] A. Kamenev and Y. Gefen, *Phys. Rev. Lett.* **114**, 156401 (2015).
- [36] R. Bhattacharyya, M. Banerjee, M. Heiblum, D. Mahalu, and V. Umansky, *Phys. Rev. Lett.* **122**, 246801 (2019).
- [37] M. Goldstein and Y. Gefen, *Phys. Rev. Lett.* **117**, 276804 (2016).
- [38] See Supplemental Material at <http://link.aps.org/supplemental/10.1103/PhysRevB.105.L081402> for details on Eqs. (1), (3), (6), (7), and (9), and more discussion on neutralon quarteting, which includes Refs. [51,52].
- [39] The chiral fields obey $[\phi_i(x), \phi_j(x')] = \pi i(\mathbf{K}^{-1})_{ij} \text{sgn}(x - x')$ [45].
- [40] T. Giamarchi and H. J. Schulz, *Phys. Rev. B* **37**, 325 (1988).
- [41] We may estimate D_{KFP} by using the RG equation $dW/d \ln D^{-1} = (3 - 2\delta)W$, where $\delta < 3/2$ is the scaling dimension and D the reduced bandwidth. At strong coupling we have $W(D_{\text{KFP}}) \sim v_0^2$, which yields $D_{\text{KFP}} \sim D_0[W(D_0)/D_0]^{1/(3-2\delta)}$ in terms of the bare bandwidth D_0 . If the KFP fixed point is not fully reached (say, at temperature $T \gtrsim D_{\text{KFP}}$) there will be RG irrelevant interactions such as $\partial_x \phi_{+,2/3,4}$, $\partial_x \phi_{-,0}$ between the charge and neutral modes.
- [42] T. Giamarchi, *Quantum Physics in One Dimension*, International Series of Monographs on Physics (Clarendon Press, Oxford, UK, 2003).
- [43] For a range of bare parameters, attraction may develop between the charge modes, in which case pairing becomes relevant [53]. Here, we assume that this is not the case.
- [44] M. Levin, *Phys. Rev. X* **3**, 021009 (2013).
- [45] I. V. Protopopov, Y. Gefen, and A. D. Mirlin, *Ann. Phys.* **385**, 287 (2017).
- [46] A. Gogolin, A. Nersisyan, and A. Tsvelik, *Bosonization and Strongly Correlated Systems* (Cambridge University Press, Cambridge, UK, 2004).
- [47] In Eq. (3), the case $\xi_t = \xi_b^*$ corresponds to equal amplitudes for creation of a right-moving (ϕ_+) neutralon pair and a left-moving (ϕ_-) antineutralon pair. In this sense, the amplitudes ξ_t and ξ_b^* correspond to the same momentum transfer.
- [48] C. L. Kane and M. P. A. Fisher, *Phys. Rev. Lett.* **72**, 724 (1994).
- [49] A. Bid, N. Ofek, M. Heiblum, V. Umansky, and D. Mahalu, *Phys. Rev. Lett.* **103**, 236802 (2009).
- [50] C. L. Kane and M. P. A. Fisher, *Phys. Rev. B* **56**, 15231 (1997).
- [51] L. Fidkowski, R. M. Lutchyn, C. Nayak, and M. P. A. Fisher, *Phys. Rev. B* **84**, 195436 (2011).
- [52] D. J. Thouless and Q. Li, *Phys. Rev. B* **36**, 4581 (1987).
- [53] J. I. Väyrynen, M. Goldstein, and Y. Gefen, *Phys. Rev. Lett.* **122**, 236802 (2019).